Effect of microstructure on the oxidation behavior of a β-solidified γ-TiAl based alloy after nitrogen ion implantation

Effect of microstructure on the oxidation behavior of a β-solidified γ-TiAl based alloy after nitrogen ion implantation

D O Panov[1], V S Sokolovsky[1*], N D Stepanov[1], S V Zherebtsov[1], V Y Novikov[1], N A Nochovnaya[2], P V Panin[2], G A Salishchev[1]
[1] Laboratory of Bulk Nanostructured Materials, Belgorod National Research University, Belgorod 308015, Russia
[2] Federal State Unitary Enterprise "All-Russian scientific research institute of aviation materials" (FSUE "VIAM"), 17 Radio str., Moscow 105005, Russia

[*]Corresponding author: sokolovskiy@bsu.edu.ru

Abstract. The microstructure of the oxide layer of a β-solidifying γ-TiAl alloy (Ti-43.2Al-1.9V-1.1Nb-1.0Zr-0.2Gd-0.2B) after nitrogen ion implantation was studied after cyclic oxidation tests at 800 ˚C. Oxidation resulted in the formation of the continuous oxide scale, consisting of thin inner and outer TiO_2, dense Al_2O_3 and mixed Al_2O_3 + TiO_2 layers. It was revealed that the nitrogen ion implantation considerably inhibited the growth of the oxide scale, internal oxidation and Al-depleted zones. Thick Al-depleted zones and a mixture of Al_2O_3 and TiO_2 were formed along the colony boundaries. Tooth-shaped Al-depleted zones propagated along the lamella boundaries. In addition, the presence of Gd-rich particles in the oxide scale promoted the formation of Al_2O_3 particles in surrounding areas and increased the depth of the oxide scale around.

1. Introduction

β-solidified gamma titanium aluminide (γ-TiAl) based alloys have attracted tremendous attention as potential high-temperature materials due to their good creep resistance and superior strength-to-weight ratio [1]. These alloys consist mainly of (α_2+γ)-lamellae colonies and have the most promising mechanical properties for aerospace engine components. However, the γ-TiAl based alloys are prone to rapid oxidation at temperatures above 600 °C, resulting in the formation of protective Al_2O_3 layer, TiO_2, a mixture of Al_2O_3 and TiO_2, inner oxide and Al-depleted zones on the surface [1-4].

It is well established that plenty of factors affect the oxide scale growth, namely the chemical composition and structure of the base material, surface finish, environment etc. [1, 5-8]. For instance, the oxidation resistance of Ti-45Al-8Nb (at.%) was considerably enhanced by the Y addition of 0.3 at.% that promoted the protective Al_2O_3 layer formation [9]. On the other hand, coarse Y_2O_3-particles, found along the grain boundaries in the alloys with high Y content (>0.3 at.%), provided fast path for the inward oxygen diffusion and significantly increased the oxidation rate [9]. Although the beneficial effects of the addition of rare-earth elements on the oxidation resistance of various alloys were known [10], there is no comprehensive understanding of the effect of Gd on the oxidation behavior of a γ-TiAl based alloy. Apart from adjusting the bulk chemical composition, surface modification, for example, by ion implantation of different non-metallic or metallic species (F, I, N, Cl, Nb, Al, Si, Mo) can effectively improve the oxidation resistance of the alloys [11-13].

The microstructure of the base material can also affect the oxidation behavior. For example, refinement of α_2-phase particles in the Ti–46Al–1Cr–0.2Si alloy inhibits oxidation dramatically [8]. Meanwhile, the orientation of lamellar colonies relative to the surface can influence the oxidation behavior of the γ-TiAl based alloys because lamellar boundaries can serve as fast diffusion pathways. However, this effect has never been properly studied. In this paper, the effect of microstructure on the oxide layer formation of a β-solidifying γ-TiAl alloy is considered.

2. Materials and methods

The β-solidifying γ-TiAl alloy with the actual composition Ti-43.2Al-1.9V-1.1Nb-1.0Zr-0.2Gd-0.2B (at. %) was used as the program material. The samples with a size of 20×20×2 mm^3 were cut from the ingots using a Sodick AQ300L wire electrical discharge machine. The samples surface was ground with emery paper up to № 2000, and then mechanically polished with an OP-S colloidal silicon suspension. The nitrogen ion implantation was produced at temperature of 400 °C in a vacuum chamber with a pressure in the range of 10^{-4} - 10^{-5} Pa. The radiation dose and ion energy were 10^{17} cm^{-2} and 40 keV, respectively.

Cyclic oxidation tests was performed in open air using a Nabertherm furnace. The samples were soaked for 24 hours at 800 °C with subsequent air cooling. After that the samples were weighed and then could be returned to the furnace again for the next test cycle. Up to 5 cycles of oxidation tests were performed.

The structure of the alloy was studied mostly using scanning electron microscopy (SEM). The following tapes of samples were tested by SEM: a beveled sample with a polished surface inclined ~5° – for the surface and material structure after nitrogen ion implantation; a cross-section of samples - for structure and element distribution of oxidation scale. The samples were examined using a FEI Quanta 600 electron microscope equipped with a back-scattered electron (BSE) and an energy-dispersive X-ray spectroscopy (EDS) detector with an accelerating voltage of 30 kV.

3. Results and discussion

The microstructure of the β-solidifying Ti-43.2Al-1.9V-1.1Nb-1.0Zr-0.2Gd-0.2B alloy consisted of (α_2+γ) lamellae colonies surrounded by γ- and (β+ω)-phase particles (Figure 1a, b). Particles of γ- and (β+ω)- phases were mainly found between the colonies. The volume fraction of γ- and (β+ω)- phase's particles was 1%. Some Gd-rich phases and a small amount of borides were found in the microstructure (Figure 1a). The volume fraction of Gd-rich particles was ≈2%. A more detailed investigation of the as-cast microstructure of the program material was presented in the previous paper [14]. The microstructure after ion implantation was presented in figure 1c. The modified layer had light grey color and depth of 1 μm; the boundary between the base material and modified layer was curved. No difference in the microstructure between the base material and modified layer was detected by SEM-BSE.

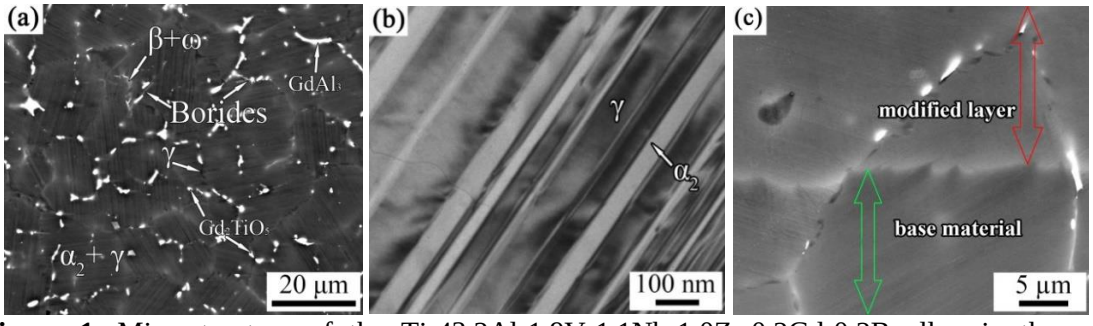

Figure 1. Microstructure of the Ti-43.2Al-1.9V-1.1Nb-1.0Zr-0.2Gd-0.2B alloy in the as-cast condition (a, b) and after ion implantation (c): (a, c) SEM-BSE images; (b) TEM image.

Figure 2 shows the growth of oxide scale and the internal oxidation and Al-depleted zones (inner zones) depth for the as-cast and nitrogen ion implanted alloy depending on the number of oxidation cycles. In this case, the internal oxidation zone referred to the oxygen-enriched aria under the oxide scale, which might also include some oxide particles. A typical example of an oxidized microstructure with identification of all layers is shown below in Figure 3. Two stages were distinguished in both conditions. At the first stage, parabolic kinetics was observed up to 3 cycles which is associated with the formation of a protective oxide layer. The formation of a protective layer led to slowing the oxide scale and inner oxide and Al-depleted zones growth at the second stage (3-5 cycles) in case of the nitrogen ion implanted alloy. After 5 cycles, the depth of the oxide scale and inner zones of the ion implanted alloy was 14 μm and 2 μm, respectively. Note that these values were considerably larger than the depth of the modified layer (~1 μm). However, almost linear growth of the oxide scale and inner oxide and Al-depleted zones for the as-cast alloy was detected at the second stage.

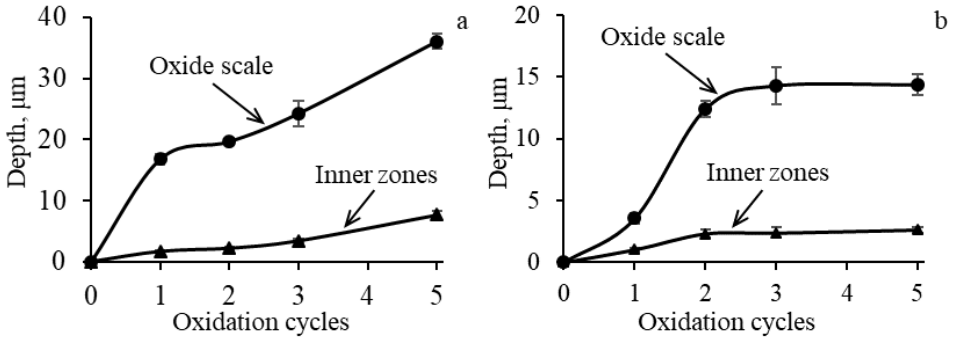

Figure 2. Dependence the depth of the oxide scale and inner zones (internal oxidation area and Al-depleted zones) of the Ti-43.2Al-1.9V-1.1Nb-1.0Zr-0.2Gd-0.2B alloy in the as-cast condition (a) and after ion implantation (b) on number of oxidation cycles at 800 °C.

The cross-section structure after 2 cycles of oxidation test is shown in Figure 3. The oxide scale mostly consisted of two oxides phases (Ti and O-rich light gray areas - TiO_2; Al and O-rich dark gray areas - Al_2O_3) [9] (Figure 2). The following layers were found: I – outward-growing TiO_2; II – Al_2O_3; III – inner TiO2; IV – a mixture of Al2O3 + TiO2; V – internal oxidation zone; VI – Al-depleted zone. The structure of the oxide scale was typical for γ-TiAl based alloys [9]. The sequence of layers depended on the ratio of outward-diffusion of Al and Ti and inward-diffusion of O on the one hand, and the ratio of the growth rate of TiO_2 and Al_2O_3, on the other hand. Obviously, TiO_2 and Al_2O_3 formed and grew simultaneously because of the similar free energy of these formation, but the growth rate of TiO_2 was drastically higher in comparison with $A1_2O_3$ [15]. Thus, the outward-growing TiO_2 layer quickly covered the surface of the material. The $A1_2O_3$ layer was found underneath the TiO_2 layer because of the diffusion of Ti toward the surface. The inner TiO_2 layer was likely formed because of the subsequent depletion of Al beneath the $A1_2O_3$ layer. The mixture of Al_2O_3+TiO_2 grew by parallel outward- and inward-diffusion [16]. As a result of the higher diffusion coefficient of Al in comparison with Ti [4], the Al-depleted zone appeared.

Thick Al-depleted zones and a mixture of Al_2O_3 and TiO_2 oxides formed along the colony boundaries. Closer look has revealed that tooth-shaped Al-depleted zones propagated along the lamella boundaries (see high resolution insert in figure 3). The presence of Gd-rich particles enhanced the formation of Al_2O_3 in surrounding areas and increased the depth of the oxide scale. Rapid diffusion of oxygen anions along colony boundaries, γ-lamellas, and Gd-rich particles can therefore increase the effective oxidation rate. It should be suggested that the noticeable positive effect of the nitrogen implantation on suppressing the oxide scale growth can be probably associated with enhancing the formation of the protective Al_2O_3 layer and, as a result, slowing the oxygen propagation. However, further studies are required to establish the oxidation mechanisms in detail.

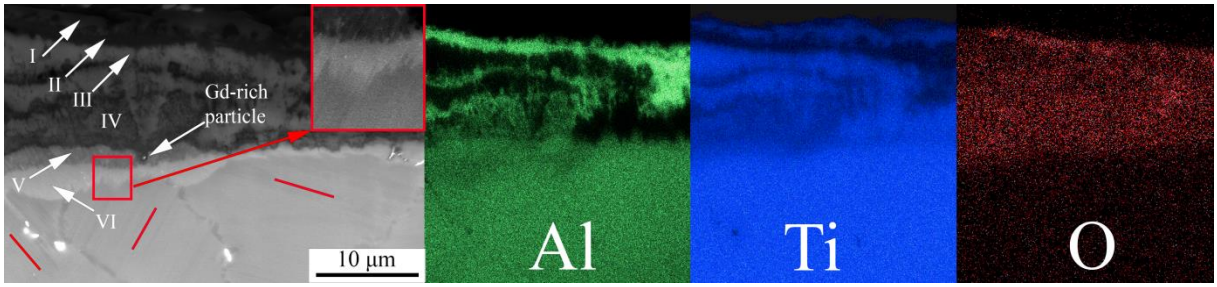

Figure 3. Cross-section SEM-BSE images and element distribution maps of the program material after nitrogen ion implantation after 2 cycles of oxidation tests. I – outward-growing TiO_2 layer; II – Al_2O_3 layer; III – inner TiO_2 layer; IV – a mixture of Al_2O_3 + TiO_2; V – internal oxidation zone; VI – Al-depleted zone; red lines indicate lamellae direction.

4. Conclusions

The dependence of the oxide scale formation on the microstructure of the base layer was studied using the example of a β-solidifying γ-TiAl alloy (Ti-43.2Al-1.9V-1.1Nb-1.0Zr-0.2Gd-0.2B) after nitrogen ion implantation. The nitrogen ion implantation improved the oxidation resistance of the alloy considerably, as was evidenced by the dependence of oxide scale thickness on number of oxidation cycles. Thick Al-depleted zones and a mixture of Al_2O_3 and TiO_2 were formed along the colony boundaries. Tooth-shaped Al-depleted zones propagated along the lamella boundaries. In addition, the presence of Gd-rich particles in the oxide scale promoted the formation of Al_2O_3 particles in surrounding areas and increased the depth of the oxide scale around.

Acknowledgment

The work was supported by the Russian Science Foundation under Grant № 19-79-30066. The authors are also grateful to Joint Research Center “Materials and Technologies”, Belgorod State University, for the assistance with instrumental analysis.

References

[1] Leyens C, Peters M 2003 *Titanium and Titanium Alloys: Fundamentals and Applications* (Weinheim: Wiley-VCH)
[2] Fergus J W 2002 *Mater. Sci. and Eng. A* **338** 108-125
[3] Tetsui T, Ono S 1999 *Intermetallics* **7** 689–697
[4] Rahmel A, Quadakkers W J, Schutze M 1995 *Mater. Corros.* **46** 271–285
[5] Zheng N, Quadakkers W J, Gil A and Nicke H 1995 *Oxidation of Metals* **44** 477-499
[6] Taniguchi S, Hongawara N, Shibata T 2001 *Materials Science and Engineering A* **307** 107–112
[7] Rakowski J M, Meier G H and Pettit F S 1996 *Scripte Materialia* **Vol. 35** 1417-1422
[8] Perez P, Jimenez J A, Frommeyer G and Adeva P 2000 *Oxidation of Metals* **Vol. 53** 138-147
[9] Zhao L L, Li G Y , Zhang L Q, Lin J P, Song X P, Ye F, Chen G L 2010 *Intermetallics* **18** 1586–1596
[10] Cueff R, Buscail H, Caudron E, Issartel C, Riffard F 2003 *Corros Sci* **45** 1815-1831
[11] Taniguchi S, Uesaki K, Zhu Y C, Fujita K, Iwamoto N, Matsunaga Y, Nakagawa K 1999 *Mater. Sci. Eng. A* **266** 267-275
[12] Hui S, Zhang Z, Xiao J, Yuan G 1999 *Rare Met.* **18 (3)** 162-167
[13] Donchev A, Schütze M 2008 *Mater Corros* **59** 489-493
[14] Sokolovsky V S, Stepanov N D, Zherebtsov S V, Nochovnaya N A, Panin P V, Zhilyakova M A, Popov A A, Salishchev G A 2018 *Intermetallics* **94** 138–151
[15] Dai J, Zhu J, Chen C, Weng F 2016 *J. Alloys Compd* **685** 784–798
[16] Becker S, Rahmel A, Schorr M, Schütze M 1992 *Oxid Met* **38** 425–464